


Article

A DFT-Based Model on the Adsorption Behavior of H_2O , H^+ , Cl^- , and OH^- on Clean and Cr-Doped Fe(110) Planes

Jun Hu ^{1,2,*} , Chaoming Wang ¹, Shijun He ¹, Jianbo Zhu ¹, Liping Wei ¹ and Shunli Zheng ^{2,*}

¹ School of Chemical Engineering, Northwest University, Xi'an 710069, China, cmwang158@163.com (C.W.); heshijun0717@163.com (S.H.); jianzhu@nwu.edu.cn (J.Z.); weiliping@nwu.edu.cn (L.W.)

² School of Materials Science and Engineering, Nanyang Technological University, 50 Nanyang Avenue, Singapore 639798, Singapore

* Correspondence: hujun32456@163.com.cn (J.H.); zhengsl@ntu.edu.sg (S.Z.); Tel.: +86-136-6928-4868 (J.H.)

Received: 1 December 2017; Accepted: 23 January 2018; Published: 29 January 2018

Abstract: The impact of four typical adsorbates, namely H_2O , H^+ , Cl^- , and OH^- , on three different planes, namely, Fe(110), Cr(110) and Cr-doped Fe(110), was investigated by using a density functional theory (DFT)-based model. It is verified by the adsorption mechanism of the abovementioned four adsorbates that the Cr-doped Fe(110) plane is the most stable facet out of the three. As confirmed by the adsorption energy and electronic structure, Cr doping will greatly enhance the electron donor ability of neighboring Fe atoms, which in turn prompts the adsorption of the positively charged H^+ . Meanwhile, the affinity of Cr to negatively charged adsorbates (e.g., Cl^- and O of H_2O , OH^-) is improved due to the weakening of its electron donor ability. On the other hand, the strong bond between surface atoms and the adsorbates can also weaken the bond between metal atoms, which results in a structure deformation and charge redistribution among the native crystal structure. In this way, the crystal becomes more vulnerable to corrosion.

Keywords: density functional theory; electron transfer; electronic structures; bond population; density of states

1. Introduction

The interaction between small molecules and metal surface is crucial in applied researches such as interfacial catalysis, anisotropic synthesis, anti-corrosion, and so forth [1]. For example, the interfacial reactions involving H_2O is significantly affected by the adsorption of H_2O molecules on the metal surface [2,3]. In addition, the adsorption of other small molecules can also greatly influence the catalytic efficiency of relative metallic catalysts, but this has been less investigated [4]. Therefore, it is paramount to understand the interaction between metal surface and various small molecules [5–7].

Quantum chemical simulation can be used to intuitively understand the geometric structure and electronic structure of metals after adsorption of H_2O . During the past few decades, considerable academic efforts have been devoted to the investigation of ion adsorption and activation over metallic iron surfaces. For example, Rafael et al. [8] studied the adsorption mechanism of a single H_2O molecule on the Fe(100) surface, which exhibited the highest adsorption energy for 0.11 and 0.25 coverages when adsorption took place on the top site of Fe. Zhao et al. [9] reported that H_2O monomers would preferentially bind to the top site and lie nearly flat on the Fe(110) surface. In addition to H_2O molecules, adsorption of H^+ and Cl^- in acidic solution also plays an important role in anti-corrosion and surface stability. Bozso et al. [10] reported the adsorption energies of H^+ on Fe(110), (100), and (111) planes, which were 26, 24, and 21 kcal/mol, respectively. Keisuke et al. [11] suggested that the small Fe clusters could form chemical bonds with gaseous H, and further absorb 10 H atoms in total by two

types of bonding mechanisms. The total magnetic moment would decrease from 4 to 0 μ_B through hydrogenation while the distance of Fe–Fe bond elongates from 2.00 to 2.79 Å. Despite the great deal of research efforts on the adsorption behavior on Fe surface, only a few have investigated the adsorption of Cl^- on surfaces of Fe and FeCr alloys, which is theoretically associated with the initiation of pitting corrosion and crack growth [12]. The comparison of different adsorbates on Fe and FeCr alloy surfaces may lead to an in-depth understanding on the anti-corrosion effect of Cr atoms.

In this study, adsorption models of aggressive species, i.e. H_2O , Cl^- , H^+ , and OH^- , on Fe(110) and Cr-doped Fe(110) facets were simulated by the quantum chemistry calculation based on density functional theory (DFT). In this comprehensive investigation which considers the adsorption energies, surface energies, bond length and population, charge transferring and density of states (DOS), we expect to reveal the impact of Cr doping on the surface properties of Fe.

2. Theoretical Calculation Methods

The DMol³ module of the Materials Studio software 8.0 (Accelrys Inc., San Diego, CA, USA) was employed for the quantum chemistry calculations. In DFT calculations, the Generalized Gradient Approximation (GGA) in the form of the Perdew–Burke–Ernzerhof (PBE) method was used for the exchange–correlation function [13–17]. The spin value was set to be unrestricted, and the formal spin was expressed as the initial value [18]. The energy convergence tolerance was higher than 1.0×10^{-5} Ha. Structures were relaxed using a geometry optimization method until the forces on all atoms were less than 0.002 Ha/Å to satisfy the convergence criterion. The double-numerical quality basis was employed, which was set with Double Numerical plus Polarization (DNP) functions. The Effective Core Potential (ECP) was used to handle the core electrons of the metallic atoms. A thermal smearing was adopted at 0.005 hartree. A Monkhorst–Pack grid of $4 \times 4 \times 1$ k point sampling in the surface Brillouin zone were used for bulk and surface calculations [19]. The k-point separation was 0.05 Å. The electron configuration of the valence was set as follows: Fe-3d⁶4s², Cr-3d⁵4s¹, O-2s²2p⁴, H-1s¹, and Cl-3s²3p⁵. During the calculations, the Fe(110) plane was chosen as the ideal model system to investigate the structure, stability, and adsorption properties because it is the most stable surface under practical conditions. A 2×2 supercell of the Fe(110) lattice structure including 4 atomic layers was constructed, and the two bottom layers were fixed. The vacuum thickness of the slab was set to 15 Å to avoid interactions between the adsorbed layer and the top layer of the bulky phase. The atomic layers and vacuum thickness were verified with small errors, as shown in Figure 1. Furthermore, the Fe(110)Cr surface was created by replacing one Fe atom in the surface center with Cr with 1/4 mL coverage. During the calculation, a top site (above the Fe atom of the central plane), a bridge site (above the location between the two Fe atoms), an hcp site (above an acute triangle of the Fe atoms of the plane), and an fcc site (above an acute triangle of the Fe atoms of the plane) takes the adsorption process into account, and the most stable adsorption site was determined by the minimum adsorption energy of the system with other pivotal properties. The bond length of Fe–Fe atoms was optimized to be 2.9627 Å on bulk Fe, which was consistent with the reported value of cubic α -Fe (JCPDS 6-0696, $a = 2.8664$ Å) [20].

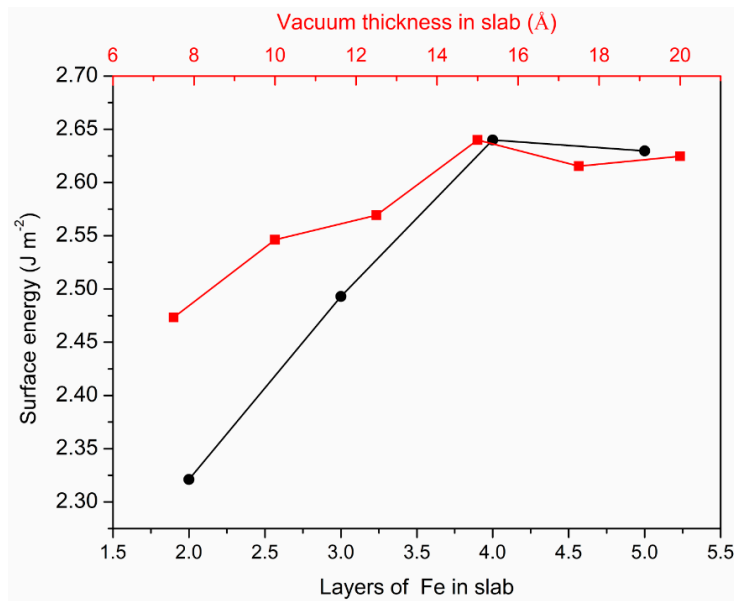


Figure 1. The surface energy of the Fe(110) slab as a function of Fe layers and vacuum using the Generalized Gradient Approximation in the form of the Perdew–Burke–Ernzerhof method (PBE-GGA) method.

3. Results and Discussion

3.1. Surface Energies Calculation

The energy of clean surface can be defined as Equation (1) [21,22].

$$\sigma_{\text{clean}} = \frac{1}{2S} (E_{\text{slab}}^N - N \times E_{\text{bulk}}) \quad (1)$$

Different adsorbate species were added to the top site for the energy calculation of the adsorbed surface. The surface energy after adsorption of different species were calculated according to the Equation (2):

$$\sigma_{\text{clean}} + \sigma_{\text{ads}} = \frac{1}{S} (E_{\text{slab}}^N - N \times E_{\text{bulk}} - nE_{\text{species}}) \quad (2)$$

where E_{slab}^N is the total electronic energy of the slab, E_{bulk} is the electronic energy of a single metal atom in the bulk, E_{species} is the optimized energy of certain species, which can be derived from the reference species including H_2O (−76.4016541 Ha), H_2 (−1.1166113 Ha), and Cl_2 (−920.121142 Ha). For example, $E_{\text{OH}^-} = E_{\text{H}_2\text{O}} - 0.5E_{\text{H}_2}$. N is the total number of atoms in the slab, and n is the total number of species on the surface. S is the surface area, and $1/2$ is applied here due to the two equal surfaces in the slab model. It should be noted that the upper and bottom surfaces must be equivalent when the slab model is created. It is clearly shown in the equations that those surfaces of low surface free energy will be more stable and vice versa. Figure 2 compared the surface energies of three different metal facets, which are calculated based on the adsorption of different species on their most stable sites.

As shown in Figure 2, the surface energy of the clean Fe(110) facet was smaller than those of the Fe(110)Cr and Cr(110) facets. The high surface energies of those surfaces indicate it is difficult to exist in reality. So both the Fe and Cr surfaces would be easy to oxidize, especially for the Cr surface. The surface energies were greatly reduced upon adsorption of H_2O , H^+ , Cl^- , and OH^- species, which suggested it is energy favorable for the process of adsorption in aqueous solution. Furthermore, the Fe(110)Cr facet showed the smallest surface energy regardless of which species was absorbed, indicating that Cr doping can strengthen adsorption.

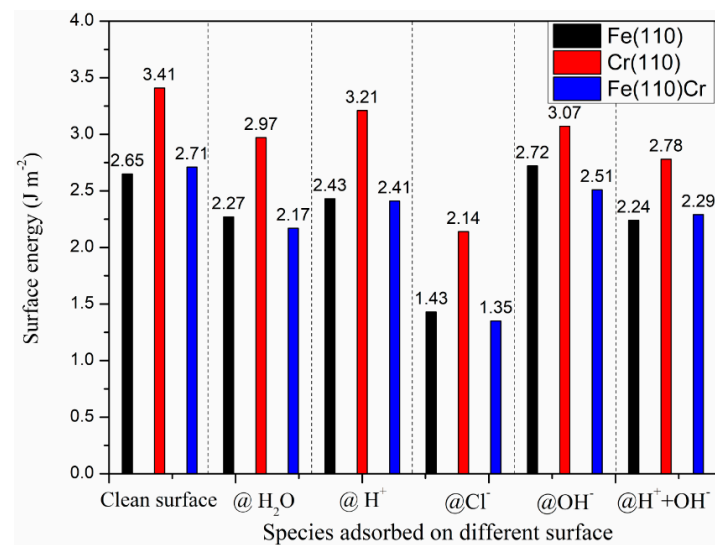


Figure 2. The calculation of surface energy for three different metal facets, based on the adsorption of different species. “@” signs stand for bond, close contact, and adsorption state on the facet.

3.2. The Most Stable Adsorption Structure of Relevant Particles

The adsorption energy (E_{ads}) between a plane and adsorbates is the key parameter in evaluating the stability of that plane [23], which can be calculated as Equation (3):

$$E_{ads} = E_{species-surface} - E_{surface} - E_{species} \quad (3)$$

where $E_{surface}$ and $E_{species-surface}$ represent the energies of metal planes before and after adsorption, respectively [24]. Theoretically, a more negative value of E_{ads} indicates a more stable adsorption between the adsorbate and the plane. The adsorption energies of four types of species binding on three facets are shown in Figure 3.

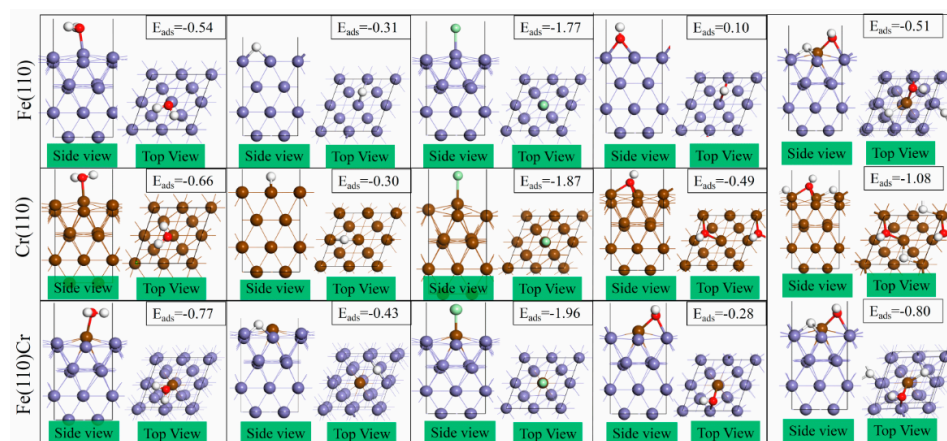


Figure 3. The geometric structures for stable adsorption of H₂O, H⁺, Cl⁻, and OH⁻ on Fe(110), Cr(110), and Fe(110)Cr planes, respectively. In the slab, purple spheres stand for Fe atoms, brown ones for Cr atoms, red ones for O atoms, green ones for Cl atoms, and white ones for H atoms. This color scheme applies to the following figures as well. The unit of E_{ads} is eV.

In the modeling, the top, bridge, hcp, and fcc sites take adsorption into account. It was found that the most stable sites for the Fe(110), Cr(110), and Fe(110)Cr surfaces were top, top, and hcp respectively, as calculated from all adsorbates taken into account. The adsorption structures were consistent with

the literature [25,26]. The geometric structures for the adsorption of each ion on different surfaces are shown in Figure 3. It can be inferred that, at the most stable site for adsorption, the alignment of H₂O molecules is parallel to the crystal surface of Fe(110)Cr, which agrees well with previous studies [27,28]. Furthermore, regarding the adsorption of H⁺, its adsorption energy on the most stable site of the Fe(110)Cr facet is more negative than those of the other two surfaces. However, the adsorption energies of H₂O and Cl[−] on the Fe(110)Cr were increased. These results preliminarily illustrated that Cr doping would greatly impact the electronic property of the neighboring Fe atoms since H⁺ was adsorbed on the neighboring Fe atoms while H₂O and Cl[−] were adsorbed on Cr atoms. The Cr doping changed the charge of neighboring Fe atoms from 0 to −0.022 e, as shown in Figure 4, and rendered them preferential for the adsorption of positively charged hydrogen. Furthermore, the highest occupied molecular orbital (HOMO) region of Cr-doped surface was mainly distributed within the Fe atom, while the lowest unoccupied molecular orbital (LUMO) region was mainly distributed within the Cr atom. Basically, the energy of the HOMO orbital is directly related to the ionization potential and characterizes the susceptibility of the molecules attacked by electrophiles. Cr doping would greatly enhance the electron donor ability of neighboring Fe atoms, which in turn would prompt the adsorption of the positively charged H⁺. Meanwhile, the affinity of Cr to negatively charged adsorbates (e.g., Cl[−] and O of H₂O, OH[−]) was improved due to the weakening of its electron donor ability.

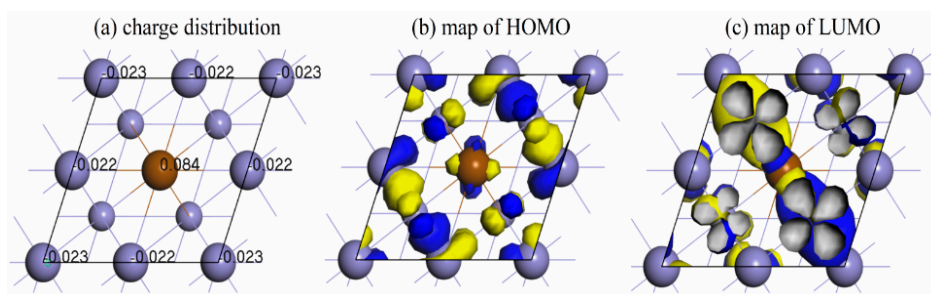


Figure 4. (a) The charge distribution on the Fe(110)Cr facets. The map of HOMO (b) and LUMO (c) in Fe(110)Cr facets, respectively. The unit of charge is e.

3.3. Density of States

DOS and partial density of states (PDOS), as shown in Figure 5, provided a more comprehensive explanation of the electronic structure [29].

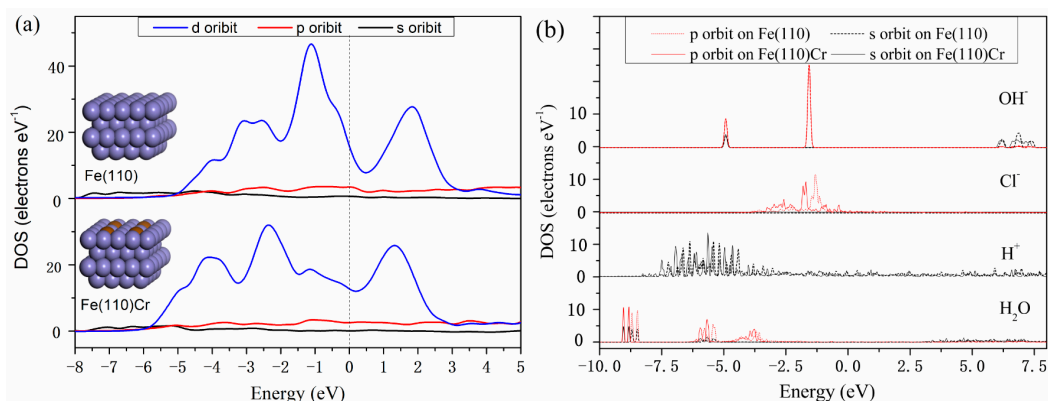


Figure 5. (a) PDOS of the Fe(110) and Fe(110)Cr facets. (b) Total DOS of H₂O, H⁺, Cl[−], and OH[−] species before and after their adsorption on Fe(110) and Fe(110)Cr facets. Each adsorbate takes the total DOS calculation into account. The data before adsorption were calculated with optimization, and the data after absorption were calculated by deleting metal atoms in the model without optimization.

As indicated in Figure 5a, the conduction of metal mainly originated from the excitation of electrons from d orbit. After Cr doping, the middle peak (from -2 eV to 0 eV) of the original Fe(110) facet showed a negative shift as well as a decrease in intensity. Figure 5b shows the PDOS of H_2O , H^+ , Cl^- , and OH^- on Fe(110) and Cr-doped Fe(110) planes. It is clearly shown that the PDOS peaks of H_2O , Cl^- , and H^+ on the Fe(110)Cr plane were shifted to a deeper energy level compared with those of the clean Fe(110) plane, which indicates a stronger bond between the Fe(110)Cr surface and the adsorbates.

3.4. The Effect Adsorbed Species on Surface

The average slab bond lengths after adsorption of H_2O , Cl^- , and H^+ on the most stable sites are presented in Figure 6.

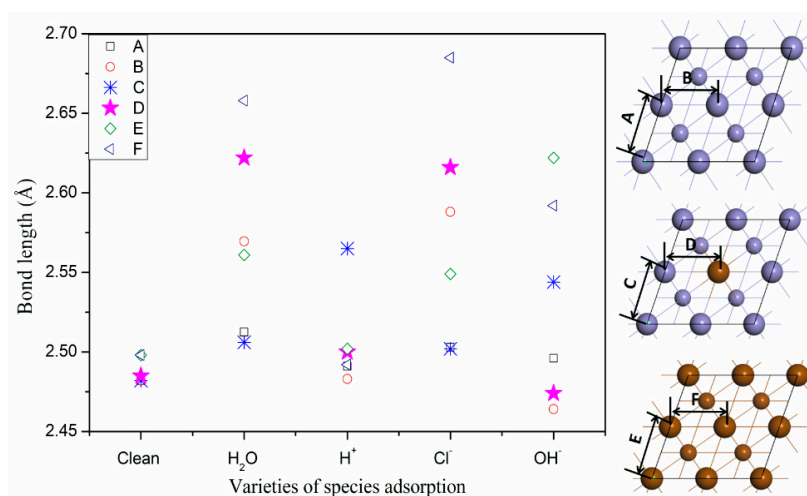


Figure 6. The change in slab bond length after adsorption of H_2O , H^+ , Cl^- , and OH^- on Fe(110) and Fe(110)Cr surfaces.

As shown in Figure 6, initially the Fe–Fe bond length on the clean Fe(110) surface was equal to that on the clean Fe(110)Cr surface. By comparing the adsorption of the four species on these three facets, it was revealed that all of the bond lengths on the three facets were greatly changed by adsorption, which confirms that the bond strength of facets can be affected by the adsorption of these four species. By comparing the bond lengths of D (as indicated in Figure 6) on the Cr-doped Fe(110) surface after adsorption of different species, it can be said that the adsorption of H_2O resulted in the most significant increase in bond length. The impact of the four species on surfaces was sorted as $\text{H}_2\text{O} > \text{Cl}^- > \text{H}^+ > \text{OH}^-$. We can conclude that, generally, the adsorbed H_2O and Cl^- will induce a greater structure deformation on surfaces, which will weaken the bond between metal atoms and render the crystal vulnerable to corrosion.

4. Conclusions

The adsorption behavior of four typical adsorbates, namely, H_2O , H^+ , Cl^- , and OH^- , on three different planes, namely, Fe(110), Cr(110), and Cr-doped Fe(110), were investigated using a DFT-based model. The surface energy study suggests that the Cr-doped Fe(110) surface is more stable than Fe(110) and Cr(110) facets upon adsorption of these four typical adsorbates. As confirmed by adsorption energy and electronic structure, Cr doping will greatly enhance the electron donor ability of neighboring Fe atoms, which in turn prompts the adsorption of the positively charged H^+ . Meanwhile, the affinity of Cr to negatively charged adsorbates (e.g., Cl^- and O of H_2O , OH^-) is improved due to the weakening of its electron donor ability. On the other hand, the strong bond between surface atoms and the adsorbates can also weaken the bond between metal atoms, which results in a structure deformation

and charge redistribution among the native crystal structure. In this way, the crystal becomes more vulnerable to corrosion.

Acknowledgments: Financial support from the National Natural Science Foundation of China (No. 21676216, 51606153), the China Postdoctoral Science Foundation (No. 2014M550507; 2015T81046), and the Innovative Projects of Northwest University (YZZ17140) is greatly acknowledged. This research project was also supported by the Center for High Performance Computing at Northwestern Polytechnical University and Haixia Ma, Northwest University, China.

Author Contributions: Jun Hu conceived and designed the simulations; Chaoming Wang and Shijun He performed the simulations; Jianbo Zhu and Liping Wei analyzed the data; Shunli Zheng wrote the paper.

Conflicts of Interest: The authors declare no conflict of interest.

References

1. Duy, D.V.; Aleksey, G.L.; Truong, K.N.; Thoi, T.N. Nitrogen trapping ability of hydrogen-induced vacancy and the effect on the formation of AlN in aluminum. *Coatings* **2017**, *7*, 79. [[CrossRef](#)]
2. Menzel, D. Water on a metal surface. *Science* **2002**, *295*, 58–59. [[CrossRef](#)] [[PubMed](#)]
3. Roman, O.; Elena, V.; Joachim, S. Water adsorption and O-defect formation on Fe₂O₃(0001) surfaces. *Phys. Chem. Chem. Phys.* **2016**, *18*, 25560–25568.
4. Magali, B.; Nathalie, T.; Joseph, M. Adsorption energy of small molecules on core-shell Fe@Au nanoparticles: Tuning by shell thickness. *Phys. Chem. Chem. Phys.* **2016**, *18*, 9112–9123.
5. Liu, X.; Kang, C.; Qiao, H.; Ren, Y.; Tan, X.; Sun, S. Theoretical studies of the adsorption and migration behavior of boron atoms on hydrogen-terminated diamond (001) surface. *Coatings* **2017**, *7*, 57. [[CrossRef](#)]
6. Lakshmi, R.V.; Bharathidasan, T.; Basu, J. Superhydrophobicity of AA2024 by a simple solution immersion technique. *Surf. Innov.* **2015**, *1*, 241–247. [[CrossRef](#)]
7. Wang, X.; Yin, X.; Nalaskowski, J.; Du, H.; Miller, J.D. Molecular features of water films created with bubbles at silica surfaces. *Surf. Innov.* **2015**, *3*, 20–26. [[CrossRef](#)]
8. Freitas, R.R.Q.; Rivelino, R.; de Brito Mota, F.; de Castilho, C.M.C. Dissociative adsorption and aggregation of water on the Fe(100) Surface: A DFT Study. *J. Phys. Chem. C* **2012**, *116*, 20306–20314. [[CrossRef](#)]
9. Zhao, W.; Wang, J.D.; Liu, F.B.; Chen, D.R. First principles investigation of water adsorption on Fe (110) crystal surface containing N. *Adv. Tribol.* **2008**, *1*, 654–657.
10. Bozsom, F.; Ertl, G.; Grunze, M.; Weiss, M. Chemisorption of hydrogen on iron surfaces. *Appl. Surf. Sci.* **1977**, *1*, 103–119. [[CrossRef](#)]
11. Keisuke, T.; Shigehito, I.; Somei, O. Chemisorption of hydrogen on Fe clusters through hybrid bonding mechanisms. *Appl. Phys. Lett.* **2013**, *102*, 11308.
12. Sun, C.; Hui, R.; Qu, W.; Yick, S. Progress in corrosion resistant materials for supercritical water reactors. *Corros. Sci.* **2009**, *51*, 2508–2523. [[CrossRef](#)]
13. Wang, H.; Nie, X.; Guo, X.; Song, C. A computational study of adsorption and activation of CO₂ and H₂ over Fe(100) surface. *J. CO₂ Utilization* **2016**, *15*, 107–114. [[CrossRef](#)]
14. Cremaschi, P.; Yang, H.; Whitten, J.L. Ab initio chemisorption studies of H on Fe(110). *Surf. Sci.* **1995**, *330*, 255–264. [[CrossRef](#)]
15. Wang, W.; Wang, G.; Shao, M. First-principles modeling of direct versus oxygen-assisted water dissociation on Fe(100) surfaces. *Catalysts* **2016**, *6*, 29. [[CrossRef](#)]
16. Hu, J.; Zhao, X.; Chen, W.; Su, H.; Chen, Z. Theoretical insight into the mechanism of photoelectrochemical oxygen evolution reaction on BiVO₄ anode with oxygen vacancy. *J. Phys. Chem. C* **2017**, *121*, 18702–18709. [[CrossRef](#)]
17. Horányi, G. Investigation of the specific adsorption of HSO₄[−] (SO₄^{2−}) and Cl[−] ions on Co and Fe by radiotracer technique in the course of corrosion of the metals in perchlorate media. *Corros. Sci.* **2004**, *46*, 1741–1749. [[CrossRef](#)]
18. Ghiasi, M.; Kamalinahad, S.; Arabieh, M.; Zahedi, M. Carbonic anhydrase inhibitors: A quantum mechanical study of interaction between some antiepileptic drugs with active center of carbonic anhydrase enzyme. *Comput. Theor. Chem.* **2012**, *992*, 59–69. [[CrossRef](#)]
19. Zhang, H. A DFT study on direct hydrogenation of amide catalyzed by a PNN Ru (II) pincer complex. *Comput. Theor. Chem.* **2015**, *1066*, 1–6. [[CrossRef](#)]

20. Kohn, W.; Sham, L.J. Self-consistent equations including exchange and correlation effects. *Phys. Rev.* **1965**, *140*, A1133. [[CrossRef](#)]
21. David, H.; Franz, D.F.; Dieter, V. Structure and surface energy of Au₅₅ nanoparticles: An *ab initio* study. *Comput. Mater. Sci.* **2017**, *134*, 137–144.
22. Ji, D.P.; Zhu, Q.X.; Wang, S.Q. Detailed first-principles studies on surface energy and work function of hexagonal metals. *Surf. Sci.* **2016**, *651*, 137–146. [[CrossRef](#)]
23. Pople, J.A.; Gill, P.M.W.; Johnson, B.G. Kohn—Sham density-functional theory within a finite basis set. *Chem. Phys. Lett.* **1992**, *199*, 557–560. [[CrossRef](#)]
24. Lanzani, G.; Laasonen, K. SO₂ and its fragments on a Cu(110) surface. *Surf. Sci.* **2008**, *602*, 321–344. [[CrossRef](#)]
25. Henderson, M.A. The interaction of water with solid surfaces: Fundamental aspects revisited. *Surf. Sci. Rep.* **2002**, *46*, 1–308. [[CrossRef](#)]
26. Hodgson, A.; Haq, S. Water adsorption and the wetting of metal surfaces. *Surf. Sci. Rep.* **2009**, *64*, 381–451. [[CrossRef](#)]
27. Xie, W.; Peng, L.; Peng, D.; Gu, F.L.; Liu, J. Processes of H₂ adsorption on Fe(110) surface: A density functional theory study. *Appl. Surf. Sci.* **2014**, *296*, 47–52. [[CrossRef](#)]
28. Michaelides, A.; Ranea, V.A.; de Andres, P.L.; King, D.A. General model for water monomer adsorption on close-packed transition and noble metal surfaces. *Phys. Rev. Lett.* **2003**, *90*. [[CrossRef](#)] [[PubMed](#)]
29. Tang, J.; Xie, K.; Liu, Y.; Chen, X.; Ma, W.; Liu, Z. Density functional theory study of leaching efficiency of acids on Si(110) surface with adsorbed boron. *Hydrometallurgy* **2015**, *151*, 84–90. [[CrossRef](#)]



© 2018 by the authors. Licensee MDPI, Basel, Switzerland. This article is an open access article distributed under the terms and conditions of the Creative Commons Attribution (CC BY) license (<http://creativecommons.org/licenses/by/4.0/>).